



Quantum criticality of U(1) gauge theories with fermionic and bosonic matter in two spatial dimensions

Ribhu K. Kaul and Subir Sachdev

Department of Physics, Harvard University, Cambridge, Massachusetts 02138, USA

(Received 17 January 2008; revised manuscript received 6 March 2008; published 3 April 2008)

We consider relativistic U(1) gauge theories in 2+1 dimensions, with N_b species of complex bosons and N_f species of Dirac fermions at finite temperature. The quantum phase transition between the Higgs and Coulomb phases is described by a conformal field theory (CFT). At large N_b and N_f , but for arbitrary values of the ratio N_b/N_f , we present computations of various critical exponents and universal amplitudes for these CFTs. We make contact with the different spin liquids, charge liquids, and deconfined critical points of quantum magnets that these field theories describe. We compute physical observables that may be measured in experiments or numerical simulations of insulating and doped quantum magnets.

DOI: [10.1103/PhysRevB.77.155105](https://doi.org/10.1103/PhysRevB.77.155105)

PACS number(s): 71.10.Hf, 11.10.Kk, 64.60.F-

I. INTRODUCTION

A number of experimental observations in the past two decades have begged for an understanding of interacting quantum systems that goes beyond the simple weakly interacting quasiparticle paradigm of solid-state physics. The large number of such systems with anomalous properties include as examples cuprate superconductors, quantum critical heavy-fermion metals,¹ Mott-insulating organic materials,² and insulating frustrated magnets.³ A paradigm that has been invoked to describe these systems is quantum number fractionalization, see, e.g., Ref. 4. Rewriting the original constituents in terms of fractional particles interacting with a gauge field and unconventional phases (or transitions) are accessed by the deconfined phases of these gauge theories. These deconfined phases cannot find a consistent description in terms of quasiparticles that are compositionally related to the particles of the microscopic description, and hence provide a paradigm that dramatically departs from the conventional confines of solid-state physics.

An important issue that arises immediately is the detection of such exotic quantum phases or phase transition in experiments or numerical simulations. In most cases, the appearance of these exotic field theories is also signaled by dramatic qualitative physical effects, e.g., a direct continuous transition between quantum states that break distinct symmetries⁵ (such a transition would not be permitted in the conventional Landau theory). While these physical effects themselves signal the appearance of the deconfined field theory, it is desirable to have a direct understanding and numerical estimate for universal quantities associated with the continuum field theories. An estimate for the universal numbers and scaling functions allows for a quantitative comparison between experiment and/or simulations and theory, and could be helpful, for instance, to distinguish between a non-universal weak first-order transition and a universal continuous one, in finite-size numerical computations.⁶⁻⁸

The starting point of our analysis will be a relativistic continuum field theory of N_f flavors of charged fermions and N_b flavors of charged bosons mutually interacting through a gauge field in two spatial dimensions. This continuum description makes no reference to the variety of microscopic

lattice models that may realize the quantum field theory. Examples of the derivations of relativistic field theoretic descriptions starting from lattice models of spins or electrons in different contexts may be found in Refs. 9–11. We postpone a discussion of the application of our results to these physical realizations to Sec. V.

We shall be interested in the general case of interacting field theories that involve bosons (z_α), Dirac fermions (Ψ_α), and gauge fields (A_μ). Working in imaginary time, the partition function of these theories may be written as functional integrals over the fields,

$$Z = \int \mathcal{D}\Psi_\alpha \mathcal{D}z_\alpha \mathcal{D}A_\mu \exp(-S_{bf}), \quad (1)$$

where the action $S_{bf} = S_b + S_f$ is specified below as the sum of bosonic and fermionic contributions.

In the field theory, the bosons are described by the complex fields, z_α , where α takes one of N_b values. The N_b fields couple through their mutual interaction with a “photon” gauge field, A_μ , in the usual minimal coupling that preserves gauge invariance.

$$S_b = \frac{N_b}{g} \int d^2r d\tau \sum_\alpha |(\partial_\mu - iA_\mu)z_\alpha|^2. \quad (2)$$

The constraint $\sum_\alpha |z_\alpha|^2 = 1$ must be satisfied at all points in time and space. The action S_b by itself is the well-known CP^{N_b-1} model. We remind the reader that in this theory, two-point correlation functions of z_α itself are “gauge-dependent” quantities, but correlation functions of the composite operator $\phi^a = z_\alpha^* T_{\alpha\beta}^a z_\beta$ are not. Indeed, the “deconfined” theory of the Néel-VBS (valence-bond solid) transition is described by S_b at $N_b=2$, and ϕ^a plays the role of the Néel order parameter where $T_{\alpha\beta}^a$ are the generators of SU(2), a physical quantity that must be gauge independent. Some large- N_b computations on this model are available in the literature.^{12,13} See Ref. 14 for a review. We will recover these results as special cases of the more general field theory of interest here.

We now turn to the action that describes the Dirac fermions. The fermionic part is described by the usual Dirac fermion action,

$$S_f = \int d^2 r d\tau \bar{\Psi}_\alpha [i\gamma^\mu (\partial_\mu - iA_\mu)] \Psi_\alpha, \quad (3)$$

where γ^μ satisfy the Clifford algebra in 2+1 dimensions, $\{\gamma^\mu, \gamma^\nu\} = 2\delta^{\mu\nu}$. We use the isotropic version of S_f , since anisotropies have been shown to be irrelevant at the critical fixed point studied here.¹⁵ We shall consider the actions S_b and S_f separately and also $S_{bf} = S_b + S_f$ in the large- N_b, N_f limit. In general, a Maxwellian term for the A_μ : $S_A = \int d^2 r d\tau (\epsilon_{\alpha\mu\nu} \partial_\mu A_\nu)^2$ should also be included. We note, however, that this term will not play an important role in our considerations: As we will show below, the contribution to the A_μ propagator from the interaction with z_α and Ψ_α at large N decays with a slow power at long distances and hence dominates the contribution from S_A at large length scales. As is usual in quantum field theory, we introduce a finite T by restricting the imaginary time integrals in the actions above to extend from 0 to $1/T$. The z_α and A_μ must then satisfy periodic and the Ψ_α antiperiodic boundary conditions.

For large enough N_f , we note here that the action S_f , when considered separately, is always quantum critical, i.e., there are no relevant perturbations consistent with its symmetry. This is in contrast to S_b which goes critical only at a single value of the coupling $g = g_c$, i.e., the boson mass is a relevant perturbation at the phase transition between the Higgs ($g < g_c$) and the deconfined Coulomb phase ($g > g_c$). The results in this paper include the results for S_f alone by simply setting $N_b = 0$. Results for the \mathbb{CP}^{N_b-1} model at criticality are obtained by setting $N_f = 0$ and the general result for finite N_b and N_f applies for the Higgs to Coulomb phase transition in the background of critical Dirac fermion excitations. We assume that A_μ is noncompact throughout this paper so that the 2+1-dimensional Coulomb phase is unequivocally stable (by definition) to monopole proliferation (see, e.g., Ref. 16). The stability of the fixed point of the combined boson-fermion action, $S_b + S_f$, using an ϵ expansion was studied in Ref. 17.

In principle, sign-problem free Monte Carlo simulations can be carried out on lattice-discretized versions of the action $S_b + S_f$. At $N_f = 0$, $N_b = 2$, the action has been simulated with a noncompact gauge field in Ref. 18 (prior simulations of a related model in the O(3) language may be found in Refs. 19 and 20). With a compact gauge field at $N_f = 0$, this field theory has been simulated²¹ for a variety of N_b . At large enough N_b , the compactness of the gauge field must be irrelevant so the criticality found in these simulations²¹ are expected to be in the same universality class as our study. Noncompact and compact QED in 2+1 dimensions have been studied in the lattice-gauge theory community (see, e.g., Ref. 22 and references therein) and are directly related to our study at $N_b = 0$; numerical results for universal quantities were, however, not presented. To our knowledge, there have been no simulations of the combined boson-fermion action, $N_b, N_f \neq 0$.

The paper is organized in the following way: In Sec. II, we first introduce the formal machinery of the large- N limit of S_{bf} considered here (large N in this paper implies large N_b, N_f but an arbitrary finite value of the ratio). In Sec. III, we then turn to an evaluation of the critical exponents and

scaling dimensions of a number of quantities of physical interest at the $T=0$ critical point that separates the Higgs from the deconfined phase in the background of massless Dirac fermions. At the critical point of S_{bf} , certain susceptibilities (corresponding to rotations in the boson or fermion flavor space) have simple linear or quadratic temperature dependencies with universal amplitudes because of conservation laws. In Sec. IV, we evaluate the numerical value of these amplitudes in the large- N limit. Finally, in Sec. V, we provide a general discussion of the physical situations in which the quantities computed in this publication may be measured in experiments or simulations of insulating and doped quantum antiferromagnets.

II. EFFECTIVE ACTION AND PROPAGATORS AT LARGE N_b, N_f

In this section, we provide the framework of the large- N_b, N_f method used here and compute the effective action at large N . At $N_b, N_f = \infty$, fluctuations of the gauge field are completely suppressed and we have a theory of free bosons and fermions. Gauge fluctuation at next-to-leading order is conveniently computed by perturbation theory, since each photon line brings a factor of $1/N$. We hence require a computation of the photon propagator at order $1/N$, in the theory S_{bf} introduced above at finite T . In this paper, we use two different gauges, depending on whether we are computing at $T=0$ or $T \neq 0$. At $T=0$, when space and time are completely interchangeable, it is convenient to use a gauge that reflects this symmetry, we use $k_\mu A_\mu$ fixed to a constant. At $T \neq 0$, for practical computation reasons, we prefer to use the gauge $k_i A_i = 0$ (with i restricted to the two space indices). Throughout this paper, we will use greek symbols α, β, μ, ν , etc., to take values x, y and τ (2+1-dimensional space time), and lowercase letters i, j , and k to take values x and y (two-dimensional space). Summation is implied on repeated indices.

A. Zero temperature

We begin with the resolution of the constraint on z_α , by introducing a real field λ , which acts as a Lagrange multiplier at each point of space and time. Then rescaling $z \rightarrow \sqrt{\frac{g}{N_b}} z$, we obtain

$$S_b = \int d^2 r d\tau \left[|(\partial_\mu - iA_\mu) z_\alpha|^2 - i\lambda \left(|z_\alpha|^2 - \frac{N_b}{g} \right) \right]. \quad (4)$$

Now, after a standard sequence of steps (see, e.g., Ref. 16) in the limit $N_b = \infty$, the gauge field drops out and λ takes on a uniform saddle point value that extremizes the action $\lambda_0 = ir$,

$$\int \frac{d^3 p}{8\pi^3} \frac{1}{p^2 + r} = \frac{1}{g}. \quad (5)$$

The propagator for the z particles is thus $G_z^{-1}(k) = k^2 + r$. At $N_b = \infty$, it becomes critical when $r=0$, i.e., at $g = g_c$ where $\frac{1}{g_c} = \int \frac{d^3 p}{8\pi^3} \frac{1}{p^2}$.

The effective action is obtained to leading order in N_b, N_f by integrating out the bosons and fermions perturbatively,

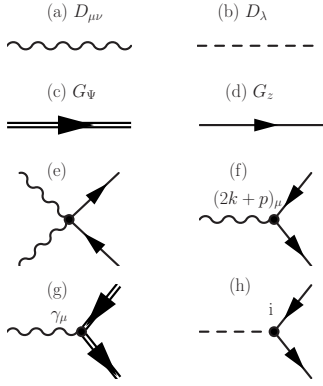


FIG. 1. Definition of diagrammatic symbols that arise from the action $S_b + S_f$. (a)–(d) illustrate the four propagators that are used to construct the various graphs used here. See Eq. (8) for the $T=0$ values and Eqs. (11) and (12) for the $T \neq 0$. (e)–(h) show the four vertices allowed by our theory and their corresponding amplitudes.

i.e., by evaluating diagrams (according to the rules of Fig. 1) that are shown in Fig. 2. At $T=0$, it is possible to obtain simple closed-form expressions for the effective action,

$$S_{A-\lambda} = \int_p \frac{\Pi_\lambda}{2} \lambda^2 + \frac{\Pi_A}{2} \left(\delta_{\mu\nu} - \frac{p_\mu p_\nu}{p^2} \right) A_\mu A_\nu, \quad (6)$$

where

$$\begin{aligned} \Pi_\lambda(p, r) &= N_b \frac{1}{4\pi p} \tan^{-1} \left(\frac{p}{2\sqrt{r}} \right), \\ \Pi_A(p, r) &= N_f \frac{p}{16} + N_b \left[\frac{p^2 + 4r}{8\pi p} \tan^{-1} \left(\frac{p}{2\sqrt{r}} \right) - \frac{\sqrt{r}}{4\pi} \right]. \end{aligned} \quad (7)$$

Details of this computation are provided in Appendix A. We note that $\Pi_\lambda(0, r) = (8\pi\sqrt{r})^{-1}$ and $\Pi_\lambda(0, 0) = \int \frac{1}{p^4}$, which is formally IR divergent in $d=3$, but this will cancel out of all physical observables.

Using the gauge $k_\mu A_\mu = 1 - \zeta$ for this $T=0$ calculation, we find the following form for the propagators:

$$\begin{aligned} D_{\mu\nu} = \langle A_\mu A_\nu \rangle &= \frac{1}{\Pi_A} \left(\delta_{\mu\nu} - \zeta \frac{q_\mu q_\nu}{q^2} \right), \\ D_\lambda = \langle \lambda \lambda \rangle &= \frac{1}{\Pi_\lambda}, \end{aligned}$$

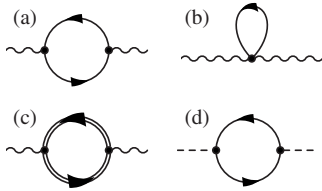


FIG. 2. One-loop diagrams that determine the effective action at large N . (a)–(c) contribute to the effective action for the A_μ and (d) contributes to the action of the λ field.

$$G_z = \langle z^* z \rangle = \frac{1}{k^2 + r},$$

$$G_\Psi = \frac{k}{k^2}, \quad (8)$$

where we have used the usual notation that $k = k^\mu \gamma^\mu$. The parameter ζ is an arbitrary gauge-fixing parameter and it should drop out of any expression for a physical observable.

B. Finite temperatures

At $T \neq 0$, there is no particular advantage in using the conventional relativistically invariant notation of Eq. (3). So we use the following equivalent form of the fermion action, designed for transparent appearance of frequency sums:

$$S_f = \int d^2x d\tau \{ \Psi_\alpha^\dagger [\partial_\tau - iA_\tau - i\sigma^x (\partial_x - iA_x) - i\sigma^y (\partial_y - iA_y)] \Psi_\alpha \}. \quad (9)$$

Again, the index $\alpha = 1 \cdots N_f$ labels the fermion flavors, Ψ_α is a two-component Dirac spinor (for each α), and $\sigma^{x,y}$ are Pauli matrices acting on the Dirac space.

The general form of the effective action for the photon at large N_b, N_f can be simply written down by invoking a Ward identity,

$$\begin{aligned} S_A = \frac{T}{2} \sum_{\epsilon_n} \int \frac{d^2k}{4\pi^2} & \left[(k_i A_\tau - \epsilon_n A_i)^2 \frac{D_1(\mathbf{k}, \epsilon_n)}{\mathbf{k}^2} \right. \\ & \left. + A_i A_j \left(\delta_{ij} - \frac{k_i k_j}{\mathbf{k}^2} \right) D_2(\mathbf{k}, \epsilon_n) \right], \end{aligned} \quad (10)$$

where D_1 and D_2 are functions that can be evaluated at large N by perturbatively integrating out both the fermions and the bosons. This process is illustrated in the Feynman graphs in Fig. 2. A complete analytic evaluation at finite T of $D_{1,2}$ is not possible. However, after some analytic manipulations detailed in Appendix A, we can bring the expressions into forms which allow efficient numerical evaluation of these functions; these evaluations will play an important role later in our $T \neq 0$ computations. In terms of $D_{1,2}$, we can immediately write down the photon propagator in the Coulomb gauge $k_i A_i = 0$. After imposing the gauge condition, the non-zero elements of the propagator are

$$D_{00}(\mathbf{q}, \epsilon_n) = \frac{1}{D_1(\mathbf{q}, \epsilon_n)},$$

$$D_{ij}(\mathbf{q}, \epsilon_n) = \left(\delta_{ij} - \frac{q_i q_j}{\mathbf{q}^2} \right) \frac{1}{D_2(\mathbf{q}, \epsilon_n) + (\epsilon_n^2 / \mathbf{q}^2) D_1(\mathbf{q}, \epsilon_n)}. \quad (11)$$

The other propagators at finite T are

$$G_z = \frac{1}{v_m^2 + \mathbf{k}^2 + r},$$

$$G_\Psi = \frac{1}{-i\omega_n + \sigma \cdot \mathbf{k}}, \quad (12)$$

where \mathbf{k} is the vector (k_x, k_y) and $\nu_m = 2\pi Tm$ and $\omega_n = 2\pi T(n + \frac{1}{2})$ are the usual bosonic and fermionic Matsubara frequencies.

III. CRITICAL EXPONENTS AND SCALING DIMENSIONS AT THE CRITICAL POINT OF S_{bf}

In this section, we will work at $T=0$ and hence use the propagators derived in Sec. II A and work in the gauge introduced there. As the coupling g is tuned, a critical point at which the condensation of z_α takes place is crossed, for small g the system enters a phase with condensed z_α and for large g the system is described by a “liquidlike” state that breaks no symmetries (here, the bosons z_α acquire a mass and the low-energy theory is a strongly coupled “algebraic” state of Dirac fermions coupled to a gauge field). In this section, we first compute two independent critical exponents associated with the singularities at this transition (ν_N and η_N), including one-loop corrections about the $N_f, N_b = \infty$ saddle point. We then turn to a calculation of the scaling dimension of the physical electron operator at the critical point.

A. Computation of ν_N in S_{bf}

We begin with the correlation length exponent, ν_N ,

$$\xi_N \propto (g - g_c)^{-\nu_N} \quad (\text{defines } \nu_N), \quad (13)$$

where ξ_N is the correlation length associated with the Néel order parameter. We note that in a given gauge, one may calculate well-defined critical exponents using z_α as the order parameter. The critical indices so calculated are in general gauge dependent. We note, however, that since the correlation length is gauge invariant so is the exponent ν_z . Hence, ν_N may be calculated without worrying about composite operators, i.e., $\nu_N = \nu_z$. Other exponents must, however, be calculated using the composite Néel field; we will present calculations for η_N in the following subsection.

We calculate the exponent of interest, ν_z , by calculating two gauge-dependent indices η_z and γ_z and then using the scaling relation $\gamma_z = \nu_z(2 - \eta_z)$. Since ν_z should be gauge independent, any dependence on the arbitrary gauge parameter ζ should drop out of the result. This is an important check on our results. We begin by defining the anomalous dimension of the z_α field as follows:

$$\dim[z_\alpha] = \frac{D-2+\eta_z}{2} \quad (\text{in a given gauge, defines } \eta_z). \quad (14)$$

We will make the gauge dependence of η_z explicit by calculating its value for arbitrary ζ . The calculation of η_z is straightforward and is obtained by picking up the coefficient of the $p^2 \log p$ pieces in a perturbative expansion of G_z , and then reexponentiating. Diagrams in Figs. 3(a) and 3(c) contribute, giving

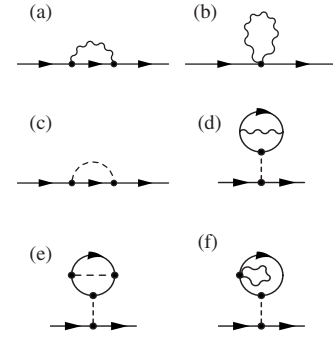


FIG. 3. Self-energy diagrams that enter the two-point z_α -boson correlation function at order $1/N$. These diagrams are evaluated in a specific gauge to extract the gauge-dependent indices η_z and γ_z . A gauge independent index ν can then be extracted from these quantities by using the exponent relation $\gamma_z = \nu_z(2 - \eta_z)$.

$$\eta_z = \frac{4}{3\pi^2 N_b} - \frac{4}{(N_f + N_b)\pi^2} \left[\frac{10}{3} + 2\zeta \right]. \quad (15)$$

For $\zeta=1$ and $N_f=0$, this reproduces the result of Ref. 12.

The critical index γ_z determines how the mass of z_α (in a given gauge) goes to zero at the critical point,

$$G_z^{-1}(k=0) = (g - g_c)^{\gamma_z} \quad (\text{defines } \gamma_z). \quad (16)$$

To leading order, we may just use $r_c = \Sigma(0,0)$ and $\frac{1}{g} = \int \frac{1}{p^2+r}$; we find

$$\frac{1}{g_c} = \int \frac{1}{p^2+r_c} = \int \frac{1}{p^2} - \int \frac{1}{p^4} \Sigma(0,0). \quad (17)$$

We introduce a new parameter r_g as follows:

$$\frac{1}{g_c} - \frac{1}{g} = \int_p \frac{1}{p^2} - \frac{1}{p^2+r_g} = \frac{\sqrt{r_g}}{4\pi}, \quad (18)$$

which can be related to r by

$$\frac{\sqrt{r_g}}{4\pi} = \frac{\sqrt{r}}{4\pi} - \int \frac{1}{p^4} \Sigma(0,0), \quad (19)$$

$$r = r_g + \frac{\Pi_\lambda(0,0)}{\Pi_\lambda(0,r)} \Sigma(0,0). \quad (20)$$

Beyond the $N_b = \infty$ approximation, the critical point is no more at $r_c=0$. In general,

$$G^{-1}(p) = (p^2 + r) - \Sigma(p,r) \quad (21)$$

and so, $r_c = \Sigma(0, r_c)$.

Now, writing the boson mass in terms of the new parameter r_g ,

$$G^{-1}(0) = r_g - \left[\Sigma(0, r_g) - \frac{\Pi_\lambda(0,0)}{\Pi_\lambda(0, r)} \Sigma(0,0) \right], \quad (22)$$

we have eliminated the quantity r completely. The goal now is to compute the term in brackets by evaluating the self-energy diagrams and pick up the terms with $r_g \log(r_g)$ diver-

gences. Then, these logs must be reexponentiated yielding the exponent γ_z as follows:

$$G^{-1}(0) = r_g \left(1 + \alpha \log \left[\frac{\Lambda^2}{r_g} \right] \right) \approx |g - g_c|^{2(1-\alpha)}, \quad (23)$$

where in the last equality we have used the fact that $r_g \propto |g - g_c|^2$, as derived above and that α vanishes in the $N \rightarrow \infty$ limit.

In order to demonstrate the usefulness of these formal manipulations, we calculate the index γ_λ for the $O(N = 2N_b)\sigma$ model. This index is of course completely gauge invariant and follows by including only the λ contributions to the self-energy, i.e., the diagrams in Figs. 3(c) and 3(e).

$$\Sigma^{(c)} = \frac{2i^2}{2!} \int \frac{d^3q}{8\pi^3} \frac{1}{\Pi_\lambda(q,r)} \frac{1}{(p+q)^2+r}, \quad (24)$$

$$\begin{aligned} \Sigma^{(e)} &= \frac{4!i^4}{4!} \frac{1}{\Pi_\lambda(0,r)} \int \frac{d^3q}{8\pi^3} \frac{1}{(q^2+r)^2} \\ &\times \int \frac{d^3p}{8\pi^3} \frac{1}{\Pi_\lambda(p,r)} \frac{1}{(p+q)^2+r}. \end{aligned} \quad (25)$$

Now, putting these expressions back into Eq. (22), we find that $\frac{\Pi_\lambda(0,0)}{\Pi_\lambda(0,r)} \Sigma(0,0) = 0$. Note, however, that this term cannot be ignored in general. Indeed, when we include gauge fluctuations below, we find that it does not evaluate to zero. In the current case, because of the vanishing of this term, we find that the quantity in brackets in Eq. (22) is simply $\Sigma^{(c)+(e)}(0,r)$,

$$= - \int \frac{d^3p}{8\pi^3} \frac{1}{\Pi_\lambda(p,r)} \left[\frac{1}{p^2+r} + \frac{\Pi'_\lambda(p,r)}{2\Pi_\lambda(0,r)} \right], \quad (26)$$

where $\Pi'_\lambda = \frac{\partial \Pi_\lambda}{\partial r}$. Now, expanding the integrand for large p , we can extract the coefficient $\alpha_\lambda = \frac{6}{\pi^2 N_b}$. Thus, $\gamma = 2 - \frac{12}{\pi^2 N_b}$, reproducing the standard result for the $O(N)$ model.²³

We now turn to the inclusion of the gauge field: There are four diagrams [Figs. 3(a), 3(b), 3(d), and 3(f)] that contribute to $\Sigma_A = \Sigma^{(a)} + \Sigma^{(b)} + \Sigma^{(d)} + \Sigma^{(f)}$. Including all factors of i^2 , contractions and factorials, they are

$$\Sigma^{(a)} = \frac{2}{2!} \int \frac{d^3q}{8\pi^3} \frac{1}{\Pi_A(q,r)} \frac{N(p,q)}{(p+q)^2+r},$$

$$\Sigma^{(b)} = (-3 + \zeta) \int \frac{d^3q}{8\pi^3} \frac{1}{\Pi_A(q,r)},$$

$$\begin{aligned} \Sigma^{(d)} &= \frac{4i^2}{2!2!} \frac{1}{\Pi_\lambda(0,r)} \int \frac{d^3q}{8\pi^3} \frac{1}{\Pi_A(q,r)} \\ &\times \int \frac{d^3p}{8\pi^3} \frac{N(p,q)}{(p^2+r)^2[(p+q)^2+r]}, \end{aligned}$$

$$\Sigma^{(f)} = \frac{(-3 + \zeta)2i^2}{2!1!} \frac{1}{\Pi_\lambda(0,r)} \int \frac{d^3p}{8\pi^3} \frac{1}{(p^2+r)^2} \int \frac{d^3q}{8\pi^3} \frac{1}{\Pi_A(q,r)}, \quad (27)$$

where $N(p,q) = 4p^2 - \frac{4\zeta}{q^2}(p \cdot q)^2 + (4p \cdot q + q^2)(1 - \zeta)$, for a general gauge. Note that generally, $\Sigma^{(b)} + \Sigma^{(f)} = 0$, so they never make an appearance.

Our task is now to compute Eq. (22) with $\Sigma = \Sigma^{(a)} + \Sigma^{(d)}$. This expression seems to be plagued with both IR and UV divergences; we will see below that both divergences exactly cancel as they must.

$$\begin{aligned} \Sigma(0,r) &= \int_q \frac{1}{\Pi_A(q,0)} \frac{q^2}{q^2+r} (1 - \zeta) \\ &- \frac{1}{\Pi_\lambda(0,r)} \int_{p,q} \frac{N(p,q)}{(p^2+r)^2[(p+q)^2+r]} \frac{1}{\Pi_A(q,r)}, \\ \Sigma(0,0) &= \int_q \frac{1}{\Pi_A(q,0)} (1 - \zeta) \\ &- \frac{1}{\Pi_\lambda(0,0)} \int_{p,q} \frac{N(p,q)}{p^4(p+q)^2} \frac{1}{\Pi_A(q,0)}. \end{aligned} \quad (28)$$

Using these in Eq. (22), we find for the term in brackets, $T_{(\dots)} = \Sigma(0,r_g) - \frac{\Pi_\lambda(0,0)}{\Pi_\lambda(0,r_g)} \Sigma(0,0)$,

$$\begin{aligned} T_{(\dots)} &= (1 - \zeta) \int_q \frac{1}{\Pi_A(q,r_g)} \frac{q^2}{q^2+r_g} \\ &- \frac{1}{\Pi_\lambda(0,r_g)} \int_{p,q} \frac{N(p,q)}{(p^2+r_g)^2[(p+q)^2+r_g]} \frac{1}{\Pi_A(q,r_g)} \\ &+ \frac{1}{\Pi_\lambda(0,r_g)} \int \left[\frac{N(p,q)}{(p+q)^2} - (1 - \zeta) \right] \frac{1}{p^4} \frac{1}{\Pi_A(q,0)}. \end{aligned} \quad (29)$$

Note that the last term was formed by combining two terms, both of which were IR divergent; this term, however, has no IR divergence. No other term has an IR divergence. We now proceed to show that all the UV divergences also exactly cancel. In order to do so, let us rewrite

$$\begin{aligned} T_{(\dots)} &= (1 - \zeta) \int_q \frac{1}{\Pi_A(q,r_g)} + (1 - \zeta) \int_q \frac{1}{\Pi_A(q,r_g)} \frac{-r_g}{q^2+r_g} \\ &- \frac{1}{\Pi_\lambda(0,r_g)} \int_q \frac{1}{\Pi_A(q,r_g)} I_A(q,r_g) \\ &+ \frac{1}{\Pi_\lambda(0,r_g)} \int \frac{1}{4q} \frac{1}{\Pi_A(q,0)}. \end{aligned} \quad (30)$$

The following integral was used on the last line: $\int_p \left[\frac{N(p,q)}{(p+q)^2} - (1 - \zeta) \right] \frac{1}{p^4} = \frac{1}{4q}$.

Now, we can rewrite this integral as

$$T_{(\dots)} = \int \frac{q^2 dq}{2\pi^2} \left[\frac{1-\zeta}{\Pi_A(q, r_g)} \frac{q^2}{q^2 + r_g} - \frac{1}{\Pi_\lambda(0, r_g)} \frac{I_A(q, r_g)}{\Pi_A(q, r_g)} + \frac{1}{\Pi_\lambda(0, r_g)} \frac{1}{4q} \frac{1}{\Pi_A(q, 0)} \right]. \quad (31)$$

All we have to do is to expand the term in $[\dots]$ for large q to extract the log divergence (evaluation of I_A is detailed in Appendix B). There should be a $O(1/q^3)$ power but all lower powers must cancel. This is indeed found to be the case

$$T_{(\dots)} = \int \frac{q^2 dq}{2\pi^2} \left[16r_g \frac{7N_f - 9N_b}{(N_b + N_f)^2} + \frac{\zeta}{N_f + N_b} \right] \frac{1}{q^3} = -\alpha_A r_g \log \left[\frac{\Lambda^2}{r_g} \right], \quad (32)$$

where $\alpha_A = -\frac{4}{\pi^2} \left[\frac{7N_f - 9N_b}{(N_b + N_f)^2} + \frac{\zeta}{N_f + N_b} \right]$.

Using $\alpha = \alpha_\lambda + \alpha_A$ and $\gamma = 2(1 - \alpha)$, we have the final expression for γ as follows:

$$\gamma = 2 - \frac{12}{\pi^2 N_b} + \frac{8}{\pi^2} \left[\frac{7N_f - 9N_b}{(N_b + N_f)^2} + \frac{\zeta}{N_f + N_b} \right]. \quad (33)$$

We note that when $\zeta = 1$, $N_f = 0$, this reduces to the result of Ref. 12 (they only present results in the Landau gauge, $\zeta = 1$). Using their quoted values of η and ν and $\gamma = \nu(2 - \eta)$, we find that their result gives (one has to also adjust N by a factor of 2, because they have a theory with $N/2$ complex fields) $\gamma = 2 - 76/(\pi^2 N_b)$, in agreement with us.

We can now calculate the coefficient ν by using a scaling relation

$$\begin{aligned} \nu_z &= \frac{\gamma_z}{2 - \eta_z} \\ &\approx \frac{\gamma}{2} \left(1 + \frac{\eta}{2} \right) \\ &\approx \left\{ 1 - \frac{6}{\pi^2 N_b} + \frac{4}{\pi^2} \left[\frac{7N_f - 9N_b}{(N_b + N_f)^2} + \frac{\zeta}{N_f + N_b} \right] \right\} \\ &\quad \times \left\{ 1 + \frac{2}{3\pi^2 N_b} - \frac{2}{(N_f + N_b)\pi^2} \left[\frac{10}{3} + 2\zeta \right] \right\} \\ &\approx 1 - \frac{16}{3\pi^2 N_b} + \frac{4}{\pi^2} \frac{7N_f - 9N_b}{(N_b + N_f)^2} - \frac{20}{(N_f + N_b)3\pi^2}. \end{aligned} \quad (34)$$

Reassuringly, the gauge parameter ζ drops out as expected. Also, for $N_f = 0$, $\nu = 1 - \frac{48}{\pi^2 N_b}$, consistent with Ref. 12.

B. Evaluation of η_N in S_{bf}

We now turn to an evaluation of the scaling dimension of the Néel field. We first define the anomalous dimension η_N through the equation

$$\dim[\phi_N^a] = \frac{D - 2 + \eta_N}{2}, \quad (35)$$

where $\phi_N^a = z_\alpha^* T_{\alpha\beta}^a z_\beta$ is the Néel field and T^a are the generators of $SU(N)$. Note that at $N_f, N_b = \infty$, the index $\eta_N = 1$, i.e., it is

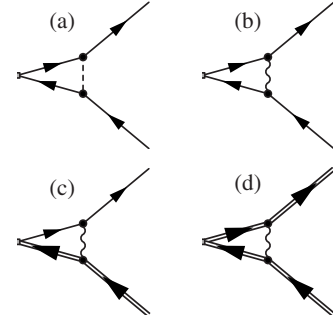


FIG. 4. Vertex corrections to the scaling dimensions for the composite operators: [(a) and (b)] Néel vector, $\phi_N^a = z_\alpha^* T_{\alpha\beta}^a z_\beta$; (c) electron operator, $c = z^* \Psi$; and (d) fermion bilinear $\Psi^\dagger \Psi$.

already nonzero. This is unlike, e.g., the $O(N)$ model, which at $N = \infty$ has no anomalous dimension. Since the Néel field is a composite of two z_α fields, its scaling dimension may be written as

$$\dim[\phi_N^a] = 2 \dim[z_\alpha] + \eta_{\text{vtx}}, \quad (36)$$

where η_{vtx} gets contributions exclusively from vertex contributions illustrated in Figs. 4(a) and 4(b). This contribution is conveniently calculated by including a source $h_a \phi_N^a$ in the action and studying its renormalization, by momentum shell renormalization group. There are two contributions coming from the photon and λ propagators (integrals are from Λ/s to Λ). They give

$$\begin{aligned} \delta h_a &= -\frac{1}{2} 2i^2 \int \frac{d^3 q}{(2\pi)^3} \frac{1}{\Pi_\lambda} \frac{1}{q^4} - \frac{1}{2} 2 \int \frac{d^3 q}{(2\pi)^3} \frac{q^2(1-\zeta)}{\Pi_A} \frac{1}{q^4} \\ &= \frac{4}{\pi^2 N_b} \log(s) - \frac{8}{\pi^2(N_f + N_b)} (1 - \zeta) \log(s). \end{aligned} \quad (37)$$

This gives $\eta_{\text{vtx}} = \frac{4}{\pi^2 N_b} - \frac{8}{\pi^2(N_f + N_b)} (1 - \zeta)$. We thus have the result

$$\eta_N = D - 2 + 2\eta_z + 2\eta_{\text{vtx}} \quad (38)$$

$$= 1 + \frac{32}{3\pi^2 N_b} - \frac{128}{3\pi^2(N_f + N_b)}. \quad (39)$$

Again, ζ drops out as expected, since η_N should be gauge invariant.

C. Scaling dimension of the electron operator at criticality

The scaling dimension of the physical electron operator is calculated at large N by identifying its scaling dimension with the bilinear $c = \bar{\Psi} z$. The scaling dimension of c must clearly be gauge invariant.

The scaling dimension of Ψ is defined by

$$\dim[\Psi] = \frac{D - 1 + \eta_\Psi}{2}. \quad (40)$$

We can evaluate η_Ψ by evaluating the lowest self-energy graph $\Sigma(k)$ due to the gauge field and then picking up the $k \log(k)$ part as follows:

$$\begin{aligned}\Sigma(k) &= \frac{2}{2!} \int \frac{d^3q}{(2\pi)^3} \frac{1}{\Pi_A} \gamma_\mu \frac{\not{q} + \not{k}}{(k+q)^2} \gamma_\nu \left(\delta_{\mu\nu} - \zeta \frac{q_\mu q_\nu}{q^2} \right) \\ &= \left[\frac{8}{3\pi^2(N_f + N_b)} - \frac{8\zeta}{\pi^2(N_f + N_b)} \right] \not{k} \log(k).\end{aligned}\quad (41)$$

This gives the gauge-dependent result $\eta_{\Psi} = \frac{8}{3\pi^2(N_b + N_f)} - \frac{8\zeta}{\pi^2(N_b + N_f)}$.

Now, we can get the gauge invariant quantity, $\dim[c]$, by including the vertex contribution in Fig. 4(c).

$$\dim[c] = \dim[z] + \dim[\Psi] + \eta_{\text{vtx}}. \quad (42)$$

The parameter ζ drops out as expected. Evaluating the vertex contribution by the momentum shell method, we find

$$\begin{aligned}\eta_{\text{vtx}} \log(s) &= \frac{-1}{1!!} \int_{\Lambda/s}^{\Lambda} \frac{d^3q}{(2\pi)^3} \frac{1}{\Pi_A} q_\mu \frac{\not{q}}{q^4} \gamma_\nu \left(\delta_{\mu\nu} - \zeta \frac{q_\mu q_\nu}{q^2} \right) \\ &= -\frac{8}{\pi^2(N_f + N_b)} (1 - \zeta) \log(s),\end{aligned}\quad (43)$$

giving the final answer

$$\dim[c] = \frac{3}{2} + \frac{2}{3\pi^2 N_b} - \frac{40}{3\pi^2(N_b + N_f)}. \quad (44)$$

Finally, we note that it is possible to construct yet another gauge invariant bilinear, $\Psi^\dagger \Psi$. Its scaling dimension, $\dim[\Psi^\dagger \Psi]$, can again be calculated for arbitrary ζ ; we find

$$\dim[\Psi^\dagger \Psi] = 2 - \frac{64}{3\pi^2(N_b + N_f)}. \quad (45)$$

This quantity too gets a vertex contribution, Fig. 4(d), in addition to the $2 \dim[\Psi]$ part. Again, the full result is reassuringly gauge invariant and for $N_b=0$ reproduces the results of Ref. 24 who calculated this number in the context of the ‘‘algebraic spin liquid.’’

IV. UNIVERSAL AMPLITUDES OF SUSCEPTIBILITIES AND SPECIFIC HEAT AT FINITE- T FROM FREE ENERGY

In the previous section, we studied the action S_{bf} at $T=0$, which corresponded to an infinite three-dimensional system. We now turn to a study of some properties at $T \neq 0$, which corresponds to studying the field theory in a slab geometry in which two dimensions are infinite, but the third direction has a finite extent of $1/T$. This naturally complicates the computations, since the relativistic invariance of $T=0$ is destroyed and frequency integrals are replaced by discrete sums on Matsubara modes. In this section, we evaluate the temperature dependence of the specific heat and certain susceptibilities that correspond to rotations among the fermionic and bosonic fields, respectively. All quantities discussed in this section may be computed exactly from the low-temperature, low-magnetic field (to be defined below) expansion of the free energy. We compute such an expansion in the large- N_b , N_f limit, allowing for an arbitrary value of the ratio N_b/N_f . Since the computations are done at finite T , we will work in

the gauge introduced in Sec. II B and use the form of the propagators derived there.

We shall consider two imaginary ‘‘magnetic fields,’’ H_b and H_f , that are applied in the ‘‘direction’’ parallel to the SU(N) generator, $\text{diag}(1 \ 1 \ \dots \ -1 \ -1 \ \dots)$. The chief advantage of using this generator is that it modifies the action in a very simple way. For the bosons, it shifts $\omega_n \rightarrow \omega_n - \theta H_b/2$, where $\theta=1$ for the first half of the components of z_α and $\theta=-1$ for the others. For the fermions, it does the same, with $\omega_n \rightarrow \omega_n - \theta H_f$.

Once we have the free energy as a function of H_b, H_f and T , we can extract the specific heat and susceptibilities by differentiating

$$\chi_b = \frac{\partial^2 \mathcal{F}}{\partial H_b^2}, \quad (46)$$

$$\chi_f = \frac{\partial^2 \mathcal{F}}{\partial H_f^2}, \quad (47)$$

$$C_V = -\frac{\partial}{\partial T} \left[T^2 \frac{\partial \mathcal{F}}{\partial T} \right] = -T \frac{\partial^2 \mathcal{F}}{\partial T^2}. \quad (48)$$

From the analysis of Ref. 25, it is known that $\chi_b, \chi_f \propto T$ and $C_V \propto T^2$. These simple integer scaling powers are due to energy conservation and bosonic and fermionic rotational symmetries. The proportionality constants of C_V, χ_b , and χ_f are universal amplitudes ($\mathcal{A}_{C_V}, \mathcal{A}_{\chi_b}$, and \mathcal{A}_{χ_f}), divided by the square of a nonuniversal velocity, c . Since c is nonuniversal, it must be determined separately for each model. In the field theoretic analysis of this section, we will set $c=1$, though its presence must be kept in mind for comparisons to simulations and/or experiments.

At large N_b and N_f , we can expand the free energy, $\mathcal{F} = -T \ln Z$,

$$\mathcal{F} = N_b f^{0b} + N_f f^{0f} + f^{1\lambda} + f^{1A} \left(\frac{N_b}{N_f} \right). \quad (49)$$

Note that in the $N=\infty$ limit, the gauge field disappears and the bosons and fermions decouple so they contribute separately; in next to leading order, this is not true. Hence, f^{0b} and f^{0f} are independent of the ratio N_b/N_f , whereas f^{1A} is a function of the ratio ($f^{1\lambda}$ can only depend on N_b and hence is also independent of the ratio N_b/N_f). In order to calculate the universal amplitudes associated with the specific heat and the susceptibilities, we compute $f^{0b}, f^{0f}, f^{1\lambda}$ and f^{1A} for arbitrary T, H_b, H_f and N_b/N_f . We first outline the computation of f^{0b}, f^{0f} and $f^{1\lambda}$, then we present the numerical results for each of χ_b, χ_f and C_V , as the ratio N_b/N_f is varied.

When $N_b, N_f = \infty$, we only need to consider a simple Gaussian theory of bosons and fermions and the computation of the free energy is straightforward. Including the shift in ω_n as discussed above, we obtain for f^{0b} and f^{0f}

$$\begin{aligned}
f^{0b} &= \frac{T}{2} \sum_{\omega_n} \int \frac{d^2k}{4\pi^2} \{ \ln[k^2 + (\omega_n + H_b/2)^2 + m^2] \\
&\quad + \ln[k^2 + (\omega_n - H_b/2)^2 + m^2] \} - \frac{m^2}{g}, \\
f^{0f} &= -T \int \frac{d^2k}{4\pi^2} \{ \ln[1 + e^{-(k+iH_f)/T}] + \ln[1 + e^{-(k-iH_f)/T}] \},
\end{aligned} \tag{50}$$

where the mass m of the bosons at the critical coupling depends only on T and the applied field H_b . It can be computed by minimizing the free energy at $N_b = \infty$. This leads to the following nonlinear equation:

$$T \sum_{\omega_n} \int \frac{d^2k}{4\pi^2} \left[\frac{1}{2k^2 + (\omega_n + \theta H_b/2)^2 + m^2} \right] = \int \frac{d^3p}{8\pi^3} \frac{1}{p^2}, \tag{51}$$

where θ should be summed over ± 1 . Applying the Poisson summation formula and evaluating the integrals and sums, we have the equation for m as follows:

$$\int \frac{d^2k}{4\pi^2} \frac{1}{2\sqrt{k^2 + m^2}} \left[\frac{1}{e^{\sqrt{k^2 + m^2 + i\theta H_b/2}/T} - 1} \right] = \frac{m}{4\pi}, \tag{52}$$

which has the solution

$$m = T \ln \left\{ \frac{2 \cos(H_b/2T) + 1 + \sqrt{[2 \cos(H_b/2T) + 1]^2 - 4}}{2} \right\}. \tag{53}$$

Computation of the various quantities of interest at $N = \infty$ follows simply by differentiating the free energy.

Turning now to the $1/N$ correction to the free energy, f_1 receives two contributions: one from the Gaussian fluctuations of the λ field and the other from the Gaussian fluctuations of A_μ . The result is

$$f^{1\lambda} = \frac{T}{2} \sum_n \int \frac{d^2k}{4\pi^2} \ln(\Pi_\lambda), \tag{54}$$

$$f^{1A} = \frac{T}{2} \sum_n \int \frac{d^2k}{4\pi^2} \ln \left(D_1 \left[D_2 + \frac{\epsilon_n^2}{k^2} D_1 \right] \right), \tag{55}$$

where Π_λ , D_1 , and D_2 are evaluated at (k, ϵ_n) , and it must be kept in mind that they depend on H_b, H_f through the shift of all internal boson and fermion frequencies (as detailed above) in the evaluation of the one-loop graphs for the λ and A_μ propagators. We note that the value of g_c gets a correction from its $N = \infty$ value, $\frac{1}{g_c} = \int \frac{d^3p}{8\pi^3} \frac{1}{p^2}$ (see Sec. II A), which can be evaluated from Eq. (21) to be $\delta \frac{1}{g_c} = \frac{4}{N_f + N_b} \int \frac{d^3q}{8\pi^3} \frac{1}{q^2}$; this shift, which is cutoff dependent, must be included in the free energy to properly cancel all the UV divergences at $O(1/N)$ and produce the universal cutoff-independent results described below.

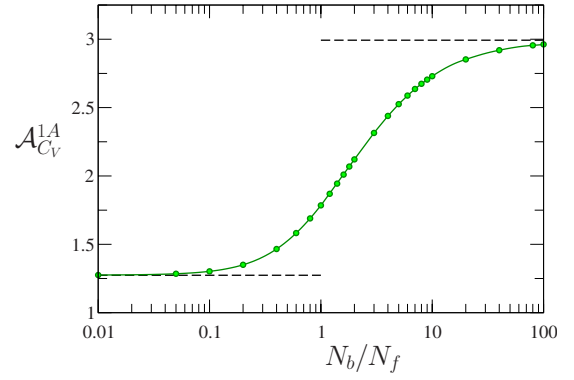


FIG. 5. (Color online) Gauge field fluctuation contribution to the specific heat amplitude, $\mathcal{A}_{C_V}^{1A}$ plotted as a function N_b/N_f . The values at $N_b/N_f = 0, \infty$ are shown for reference as dashed lines.

We now turn to a presentation of our results for C_V, χ_b , and χ_f , obtained by numerically differentiating computations of the free energy formulas outlined above.

A. Specific heat

The quantum critical specific heat at low T is of the form $C_V = \mathcal{A}_{C_V} T^2$, where we can organize the large- N expansion of the universal amplitude \mathcal{A}_{C_V} as

$$\mathcal{A}_{C_V} = N_b \mathcal{A}_{C_V}^{0b} + N_f \mathcal{A}_{C_V}^{0f} + \mathcal{A}_{C_V}^{1\lambda} + \mathcal{A}_{C_V}^{1A}(N_b/N_f). \tag{56}$$

Differentiating Eq. (50), we obtain the estimates $\mathcal{A}_{C_V}^{0b} = 6 \frac{8\zeta(3)}{10\pi} \approx 1.83661$ and $\mathcal{A}_{C_V}^{0f} = 6 \frac{3\zeta(3)}{4\pi} \approx 1.72182$. Note that the proportionality of $\mathcal{A}_{C_V}^{0b}$ to $\zeta(3)$ with a rational coefficient is nontrivial.²⁶

Turning to the $1/N$ corrections, the computations of $\mathcal{A}_{C_V}^{1\lambda}$ and $\mathcal{A}_{C_V}^{1A}$ are far more complicated and involve some tedious numerical calculations. Basically, numerical computations of the finite temperature propagators (as detailed in Appendix A) have to be inserted into Eq. (54), which is then itself evaluated numerically. From our numerical analysis, we obtain $\frac{T}{2} \sum_n \int \frac{d^2k}{4\pi^2} \ln[8\sqrt{k^2 + \epsilon_n^2} \Pi(k, \epsilon_n)] = -0.03171T^3$, allowing us to estimate $\mathcal{A}_{C_V}^{1\lambda} = -0.38368$. We can get $\mathcal{A}_{C_V}^{1A}$ from a similar analysis; we plot it as a function of N_b/N_f in Fig. 5.

B. Susceptibility to applied H_b

The susceptibility to H_b is obtained by differentiating the free energy twice with respect to H_b (keeping $H_f = 0$ throughout). The large- N expansion of the amplitude \mathcal{A}_{χ_b} defined from $\chi_b = \mathcal{A}_{\chi_b} T$ can be organized as

$$\mathcal{A}_{\chi_b} = N_b \mathcal{A}_{\chi_b}^{0b} + \mathcal{A}_{\chi_b}^{1\lambda} + \mathcal{A}_{\chi_b}^{1A}(N_f/N_b). \tag{57}$$

We obtain the estimate $\mathcal{A}_{\chi_b}^{0b} = \frac{\sqrt{5}}{4\pi} \ln\left(\frac{\sqrt{5}+1}{2}\right) \approx 0.0856271$. From our numerical analysis described briefly above, we find $\frac{T}{2} \sum_n \int \frac{d^2k}{4\pi^2} \ln[8\sqrt{k^2 + \epsilon_n^2} \Pi(k, \epsilon_n)] = -0.03171T^3 - 0.01325H_b^2T$. This allows us to estimate $\mathcal{A}_{\chi_b}^{1\lambda} \approx -0.02650$. Finally, from the numerical evaluation of the gauge field, we plot the function $\mathcal{A}_{\chi_b}^{1A}(N_f/N_b)$ in Fig. 6.

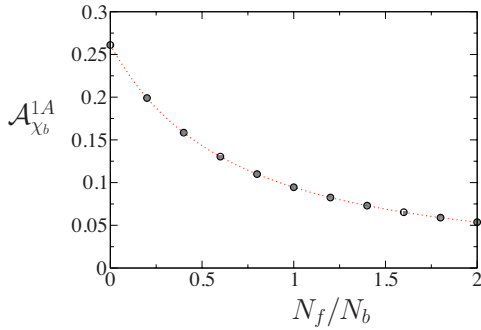


FIG. 6. (Color online) Gauge field contribution to the amplitude of the susceptibility to applied H_b as a function of N_f/N_b .

C. Susceptibility to applied H_f

Finally, we turn to an evaluation of the susceptibility to H_f which also has a linear- T dependence. The universal amplitude appearing (just as in the case of χ_b above) can be expanded as

$$\mathcal{A}_{\chi_f} = N_f \mathcal{A}_{\chi_f}^{0f} + \mathcal{A}_{\chi_f}^{1A}(N_b/N_f). \quad (58)$$

In this case, we obtain $\mathcal{A}_{\chi_f}^{0f} = 2 \frac{\ln(2)}{2\pi} \approx 0.220636$. A computation of the function $\mathcal{A}_{\chi_f}^{1A}(N_b/N_f)$ along the lines described above is plotted in Fig. 7.

V. CONCLUSIONS

All the computations carried out in this paper have been for the continuum field theory, S_{bf} , and are hence of interest to any problem which realizes this field theoretic description. We now list three different physical problems of interest to which these results are applicable, and provide a brief summary of the connections between physical quantities and the universal numbers we have computed. Another context in which the thermodynamics of the S_{bf} theory appears is the QED₃ theory of underdoped cuprates.²⁷ We note that the “magnetic” susceptibility considered in Ref. 27 is not a correlation function of generators of the flavor symmetry (as we have calculated here). Hence, while our results for the specific heat apply to their model, their magnetic susceptibility is distinct from our χ_f .

Deconfined Néel-VBS transition. The deconfined Néel-

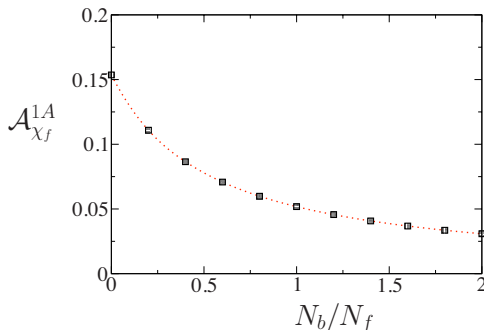


FIG. 7. (Color online) Gauge field contribution to the amplitude of the susceptibility to applied H_f as a function of N_b/N_f .

VBS transition has been shown to be described by the field theory S_{bf} with $N_f=0$. The results of Sec. III apply directly to the critical exponents of this transition (which has $N_f=0, N_b=2$). In particular, Eqs. (34) and (38) characterize the two-point Néel correlation function. At the Néel-VBS quantum critical point, the uniform magnetic susceptibility, χ_u , should depend linearly on temperature. This quantity is exactly the χ_b , Eq. (57) computed in Sec. IV with $N_f=0$. The result for C_V , Eq. (56) with $N_f=0$ also applies to the deconfined Néel-VBS transition.

Algebraic charge liquids. In a recent publication,¹¹ a new class of states of matter, dubbed “algebraic charge liquids” (ACLs), were shown to arise naturally in doped quantum antiferromagnets, which are close to the deconfined Néel-VBS quantum critical point. In the language of this study, z_α are bosons that carry spin and Ψ are the superconducting quasiparticles. In this study, the transition from a superconducting Néel state to the superconducting ACL state is described precisely by the field theory under study here with $N_b=2$ and $N_f=4$, whereas the criticality of the ACL state is described simply by $N_b=0, N_f=4$. The critical exponents of Sec. III apply directly to the transition from the superconducting Néel state to the s-ACL state. It has been shown¹¹ that the susceptibility χ_f discussed in Sec. IV is related to the finite- T contribution to the superfluid density of the s-ACL state (the result for χ_f at $N_b=0$ was published in Ref. 11). Just like the Néel-VBS case, the susceptibility χ_b is the uniform magnetic susceptibility, and in Sec. IV, we have the results for the universal amplitude both at the critical point and in the s-ACL phase.

Algebraic spin liquids. Finally, the result for χ_f with $N_b=0$ applies to the fermionic spin theories of algebraic spin liquids of square,²⁸ kagome,²⁹ and other lattices. In this case, χ_f is related to the uniform magnetic spin susceptibility because the fermions carry spin.

ACKNOWLEDGMENTS

The authors thank Y. Kim, T. Senthil, and Z. Tesanovic for valuable discussions. This research was supported by NSF Grants No. DMR-0537077 (S.S. and R.K.K.), No. DMR-0132874 (R.K.K.), and No. DMR-0541988 (R.K.K.). R.K.K. and S.S. acknowledge the hospitality of “Aspen Center for Physics” where part of this research was carried out.

APPENDIX A: EFFECTIVE ACTION AT LARGE N : EVALUATION OF D_1 , D_2 , Π_A , AND Π_λ

In this section, we provide the details on the evaluation of the functions D_1 and D_2 that determine the effective action for the photons at large N . We evaluate the general form of these functions at large N_b, N_f and at finite T , as defined in Eq. (10). From these results, we can get Π_A relevant to Sec. II A, by setting $T=0$ and completing all integral analytically. Finally, we provide a computation of the λ propagator.

The evaluation of D_1 and D_2 corresponds to evaluating the diagrams in Fig. 2 at finite T . Each function gets a contribution from the bosonic as well as fermionic loops. We evaluated these separately, writing $D_1 = D_{1b} + D_{1f}$ and D_2

$=D_{2b}+D_{2f}$. We first present an evaluation of the fermionic loops and then turn to a computation of the bosonic contributions.

1. D_{1f}, D_{2f} : Fermionic loops

The only diagram that needs to be evaluated for the fermions is the one appearing in Fig. 2(c). Starting with the function $D_{1f}(k, \epsilon_n)$ we have

$$\begin{aligned} D_{1f}(k, \epsilon_n) &= -N_f \int_{\mathbf{q}, \omega_n} \text{Tr}[G_\Psi(\mathbf{q}, \omega_n)G_\Psi(\mathbf{k} + \mathbf{q}, \omega_n + \epsilon_n)] \\ &= 2N_f \int_{\mathbf{q}, \omega_n} \frac{\omega_n(\omega_n + \epsilon_n) - \mathbf{q} \cdot (\mathbf{q} + \mathbf{k})}{(\omega_n^2 + q^2)[(\omega_n + \epsilon_n)^2 + (\mathbf{q} + \mathbf{k})^2]} \\ &= N_f \int_{\mathbf{q}, \omega_n} \left\{ \frac{-2}{q^2 + \omega_n^2} \right. \\ &\quad \left. + \frac{(2\omega_n + \epsilon_n)^2 + k^2}{(\omega_n^2 + q^2)[(\omega_n + \epsilon_n)^2 + (\mathbf{q} + \mathbf{k})^2]} \right\}. \end{aligned} \quad (\text{A1})$$

We will use the shorthand $\int_{\mathbf{q}, \omega_n} = T \sum_{\omega_n} \int \frac{d^d q}{4\pi^2}$ to signify a summation on the internal frequencies and momenta in this paper. Evaluating the first term by ζ -function regularization, and performing the momentum integration in the second term using the usual Feynman trick, we find

$$\begin{aligned} D_{1f}(\mathbf{k}, \epsilon_n) &= \frac{N_f T \ln 2}{\pi} + \frac{N_f T}{4\pi} \\ &\quad \times \sum_{\omega_n} \int_0^1 dx \frac{(2\omega_n + \epsilon_n)^2 + \mathbf{k}^2}{(1-x)\omega_n^2 + x(\omega_n + \epsilon_n)^2 + \mathbf{k}^2 x(1-x)} \\ &= \frac{N_f T \ln 2}{\pi} + \frac{N_f T}{4\pi} \sum_{\omega_n} 2 \frac{(2\omega_n + \epsilon_n)^2 + \mathbf{k}^2}{A} \\ &\quad \times \ln \frac{A + \mathbf{k}^2 + \omega_n^2 + (\omega_n + \epsilon_n)^2}{2|\omega_n(\omega_n + \epsilon_n)|}, \end{aligned}$$

where

$$A^2 = [\mathbf{k}^2 + (|\omega_n| - |\omega_n + \epsilon_n|)^2][\mathbf{k}^2 + (|\omega_n| + |\omega_n + \epsilon_n|)^2]. \quad (\text{A2})$$

The frequency summation is formally divergent, but we can subtract the divergent piece by ζ -function regularization to yield

$$\begin{aligned} D_{1f}(\mathbf{k}, \epsilon_n) &= \frac{N_f T \ln 2}{\pi} + \frac{N_f T}{4\pi} \sum_{\omega_n} \left\{ 2 \frac{(2\omega_n + \epsilon_n)^2 + \mathbf{k}^2}{A} \right. \\ &\quad \left. \times \ln \frac{A + \mathbf{k}^2 + \omega_n^2 + (\omega_n + \epsilon_n)^2}{2|\omega_n(\omega_n + \epsilon_n)|} - 4 \right\}. \end{aligned} \quad (\text{A3})$$

This frequency summation is now evaluated numerically. For this, it is useful to know the large ω_n behavior of the term in the curly brackets. After symmetrizing the positive and negative frequencies, we obtain

$$(\mathbf{k}^2 + \epsilon_n^2) \left[\frac{1}{3\omega_n^2} + \frac{9\epsilon_n^2 - \mathbf{k}^2}{30\omega_n^4} + \frac{50\epsilon_n^4 - 19\epsilon_n^2 \mathbf{k}^2 + \mathbf{k}^4}{210\omega_n^6} + \dots \right]. \quad (\text{A4})$$

The asymptotic behavior is then summed by using the identities

$$\begin{aligned} \sum_{n=N+1}^{\infty} \frac{1}{(2n-1)^2} &= \frac{1}{4N} - \frac{1}{48N^3} + \frac{7}{960N^5} + \dots, \\ \sum_{n=N+1}^{\infty} \frac{1}{(2n-1)^4} &= \frac{1}{48N^3} - \frac{1}{96N^5} + \dots, \\ \sum_{n=N+1}^{\infty} \frac{1}{(2n-1)^6} &= \frac{1}{320N^5} + \dots. \end{aligned} \quad (\text{A5})$$

We now turn to a similar evaluation as above for D_{2f} ,

$$\begin{aligned} D_{2f}(k, \epsilon_n) &= -\frac{\mathbf{k}^2}{k_x k_y} NT \sum_{\omega_n} \int \frac{d^d q}{4\pi^2} \text{Tr}[\sigma_x G_\Psi(\mathbf{q}, \omega_n) \sigma_y G_\Psi(\mathbf{k} + \mathbf{q}, \omega_n + \epsilon_n)] \\ &= -\frac{\mathbf{k}^2}{k_x k_y} 2NT \sum_{\omega_n} \int \frac{d^d q}{4\pi^2} \frac{2q_x q_y + q_x k_y + q_y k_x}{(\omega_n^2 + \mathbf{q}^2)[(\omega_n + \epsilon_n)^2 + (\mathbf{q} + \mathbf{k})^2]} \\ &= \frac{N_f T}{\pi} \int_0^1 dx \sum_{\omega_n} \frac{x(1-x)\mathbf{k}^2}{[(1-x)\omega_n^2 + x(\omega_n + \epsilon_n)^2 + \mathbf{k}^2 x(1-x)]} \\ &= \frac{N_f T}{\pi} \sum_{\omega_n} \left\{ 1 + \frac{(\omega_n + \epsilon_n)^2 - \omega_n^2}{2\mathbf{k}^2} \ln \frac{(\omega_n + \epsilon_n)^2}{\omega_n^2} - \frac{[(\omega_n + \epsilon_n)^2 - \omega_n^2]^2 + \mathbf{k}^2[(\omega_n + \epsilon_n)^2 + \omega_n^2]}{A\mathbf{k}^2} \ln \frac{[A + \mathbf{k}^2 + \omega_n^2 + (\omega_n + \epsilon_n)^2]}{2|\omega_n(\omega_n + \epsilon_n)|} \right\}. \end{aligned} \quad (\text{A6})$$

The large ω_n behavior of the term in the curly brackets, after symmetrizing the positive and negative frequencies, is

$$\mathbf{k}^2 \left[\frac{1}{6\omega_n^2} + \frac{7\epsilon_n^2 - 2\mathbf{k}^2}{60\omega_n^4} + \frac{13\epsilon_n^4 - 34\epsilon_n^2\mathbf{k}^2 + 3\mathbf{k}^4}{420\omega_n^6} + \dots \right]. \quad (\text{A7})$$

At $T=0$, the exact values of $D_{1,2f}$ can be computed analytically,

$$D_{1f}(\mathbf{k}, \omega) = D_{2f}(\mathbf{k}, \omega) = \frac{N_f \mathbf{k}^2}{16\sqrt{\mathbf{k}^2 + \omega^2}}. \quad (\text{A8})$$

2. D_{1b}, D_{2b} : Bosonic loops

We now present the evaluation of D_{1b} and D_{2b} that arise from the diagrams in Figs. 2(a) and 2(b). The function D_{1b} is

$$D_{1b}(\mathbf{k}, \epsilon_n) = N_b T \sum_{\omega_n} \int \frac{d^2 q}{4\pi^2} \left\{ \frac{2}{\mathbf{q}^2 + \omega_n^2 + r} - \frac{(2\omega_n + \epsilon_n)^2}{(\mathbf{q}^2 + \omega_n^2 + r)[(\mathbf{q} + \mathbf{k})^2 + (\omega_n + \epsilon_n)^2 + r]} \right\}. \quad (\text{A9})$$

The first term we evaluate by dimensional regularization

$$= T \sum_{\omega_n} \int \frac{d^d q}{4\pi^2} \frac{2}{\mathbf{q}^2 + \omega_n^2 + r} \quad (\text{A10})$$

$$\begin{aligned} &= \frac{\Gamma(1-d/2)}{(4\pi)^{d/2}} T \sum_n \frac{1}{(\omega_n^2 + r)^{1-d/2}} \\ &= \frac{\Gamma(1-d/2)}{(4\pi)^{d/2}} T^{d-1} \left[\left(\frac{T}{\sqrt{r}} \right)^{2-d} + (d-2) \sum_{n=1}^{\infty} \ln \left(1 + \frac{r}{\omega_n^2} \right) \right. \\ &\quad \left. + \frac{2}{(2\pi)^{2-d}} \zeta(2-d) \right] \end{aligned} \quad (\text{A11})$$

$$= -\frac{1}{2\pi} \left[\ln \left(\frac{\sqrt{r}}{T} \right) + \sum_{n=1}^{\infty} \ln \left(1 + \frac{r}{\omega_n^2} \right) \right] = 0, \quad (\text{A12})$$

where we have used the large- N value for the mass parameter $\sqrt{r} = 2 \ln[(\sqrt{5}+1)/2]$ in the last line (see Chap. 5 of Ref. 30 for more details).

$$D_{1b}(\mathbf{k}, \epsilon_n) = \frac{N_b T}{4\pi} \sum_{\omega_n} \int_0^1 dx \left[4 - \frac{(2\omega_n + \epsilon_n)^2}{(1-x)\omega_n^2 + x(\omega_n + \epsilon_n)^2 + r + \mathbf{k}^2 x(1-x)} \right]. \quad (\text{A13})$$

The frequency summand has the following expansion at large ω_n :

$$\begin{aligned} &\frac{2\mathbf{k}^2 + 12r - \epsilon_n^2}{3\omega_n^2} + \frac{-4\mathbf{k}^4 + \mathbf{k}^2(-40r + 17\epsilon_n^2) - 3(40r^2 - 50r\epsilon_n^2 + 3\epsilon_n^4)}{30\omega_n^4} \\ &+ \frac{6\mathbf{k}^6 + (84r - 73\epsilon_n^2)\mathbf{k}^4 + (420r^2 - 826\epsilon_n^2 r + 81\epsilon_n^4)\mathbf{k}^2 + 10(84r^3 - 315\epsilon_n^2 r^2 + 147\epsilon_n^4 r - 5\epsilon_n^6)}{210\omega_n^6}. \end{aligned}$$

For D_{2b} we have

$$D_{2b}(\mathbf{k}, \epsilon_n) = \frac{N_b T}{4\pi} \sum_{\omega_n} \int_0^1 dx \frac{\mathbf{k}^2(2x-1)^2}{(1-x)\omega_n^2 + x(\omega_n + \epsilon_n)^2 + r + \mathbf{k}^2 x(1-x)}, \quad (\text{A14})$$

and the following expansion at large ω_n :

$$\begin{aligned} &\mathbf{k}^2 \left[\frac{1}{3\omega_n^2} - \frac{\mathbf{k}^2 + 10r - 11\epsilon_n^2}{30\omega_n^4} \right. \\ &\quad \left. + \frac{\mathbf{k}^4 + 70r^2 - 266r\epsilon_n^2 + 86\epsilon_n^4 + 14\mathbf{k}^2 r - 23\mathbf{k}^2 \epsilon_n^2}{210\omega_n^6} \right]. \end{aligned} \quad (\text{A15})$$

3. Π_A and Π_λ : Action at $T=0$

The above expressions for D_1 and D_2 at finite T were brought into a form from which efficient numerical evaluation was possible. At $T=0$, a full analytic evaluation of the integrals entering the effective action is possible. We will outline the steps of these calculations now. We begin with a computation of Π_A . Just as in the finite- T case, $\Pi_A = \Pi_A^b + \Pi_A^f$ receives contribution from both bosonic and fermionic loops, which follow from the $T \rightarrow 0$ limit of the above

expressions for the finite- T action. Using the form in Eq. (6), we can deduce by looking, for example, at the $q_x q_y$ term as follows:

$$-\Pi_A^b \frac{q_x q_y}{q^2} = -N_b \int \frac{d^3 q}{8\pi^3} \frac{(2k+q)_x (2k+q)_y}{(k^2+r)[(k+q)^2+r]}. \quad (\text{A16})$$

Now, the evaluation of this integral follows the standard steps (outlined, for example, in Appendix B) and we find

$$\Pi_A^b(p, r) = N_b \left[\frac{p^2 + 4r}{8\pi p} \tan^{-1} \left(\frac{p}{2\sqrt{r}} \right) - \frac{\sqrt{r}}{4\pi} \right]. \quad (\text{A17})$$

The fermionic contribution can be evaluated in a similar way or by noting the simple relationship, $\Pi_A = \frac{p^2 + \omega^2}{p^2} D_2(\mathbf{p}, \omega)$, giving from Eq. (A8) that

$$\Pi_A^f(p) = \frac{N_f p}{16}. \quad (\text{A18})$$

Putting these results together we get the expression for Π_A quoted in Eq. (7). It is curious to note that when $r=0$ the bosonic contribution becomes $\Pi_A^b(p, 0) = \frac{N_b p}{16}$, exactly the same as for the fermions.

The evaluation of Π_λ follows the same steps as for Π_A^b except with different contributions at the vertices, Fig. 2(d).

$$\Pi_\lambda(q) = N_b \int \frac{d^3 k}{8\pi^3} \frac{1}{(k^2+r)[(k+q)^2+r]}, \quad (\text{A19})$$

which can be evaluated using the usual Feynman parameter and integration shift of Appendix B, resulting in the form quoted in Eq. (7).

APPENDIX B: EVALUATION OF I_A

Here, we explicitly show how to calculate I_A that appears in computations of Sec. III A. We note that we have used the standard sequence of steps illustrated in this example below many times in the course of the computations presented in this paper.

$$I_A = \int \frac{d^3 p}{8\pi^3} \frac{4p^2 - \frac{4\zeta}{q^2}(p \cdot q)^2 + (4p \cdot q + q^2)(1-\zeta)}{(p^2 + r_g)^2 [(p+q)^2 + r_g]}. \quad (\text{B1})$$

The integral is evaluated by executing the following steps in sequence: Introduce a Feynman parameter x , shift to $l=p+xq$, integrate over l , and then integrate over x .

$$\begin{aligned} I_A &= \int_0^1 dx 2(1-x) \\ &\times \int \frac{d^3 p}{8\pi^3} \frac{4p^2 - \frac{4\zeta}{q^2}(p \cdot q)^2 + (4p \cdot q + q^2)(1-\zeta)}{\{(1-x)(p^2 + r_g) + x[(p+q)^2 + r_g]\}^3} \\ &= \int_0^1 dx 2(1-x) \end{aligned}$$

$$\begin{aligned} &\times \int \frac{d^3 l}{8\pi^3} \frac{4l^2 \left(1 - \frac{\zeta}{3}\right) + q^2(1-\zeta)[4x(x-1) + 1]}{[l^2 + r + q^2 x(1-x)]^3} \\ &= \int_0^1 dx 2(1-x) \left\{ \frac{3}{8\pi} \frac{1-\zeta/3}{\sqrt{q^2(1-x)x+r}} \right. \\ &\quad \left. + \frac{[4x(x-1) + 1](1-\zeta)q^2}{32\pi} \frac{1}{[\sqrt{q^2(1-x)x+r}]^3} \right\} \\ &\approx (1-\zeta)\Pi_\lambda(0, r_g) + \frac{1}{4q} - \frac{\sqrt{r_g}}{\pi q^2} + \mathcal{O}\left(\frac{1}{q^3}\right). \quad (\text{B2}) \end{aligned}$$

The neglected terms produce UV convergent diagrams when the integrals over q are evaluated and hence can be neglected.

APPENDIX C: DIAGRAMMATIC EVALUATION OF FERMION SUSCEPTIBILITY

In this appendix, we calculate one of the universal amplitudes of Sec. IV, \mathcal{A}_{χ_f} by an entirely different diagrammatic method. The perfect agreement between the two methods provides a nontrivial check on our rather involved computations.

Consider the susceptibility, χ_f , of the $SU(N_f)$ charge, $Q^a = \Psi_{\alpha\beta}^\dagger T_{\alpha\beta}^a \Psi_\beta$, where T^a is a generator of the symmetry. Since the $SU(N_f)$ charge is a conserved density, it acquires no anomalous dimension. Indeed, a simple scaling analysis²⁵ establishes that for $z=1$ criticality, in $d=2$ spatial dimensions, it must have a linear- T dependence with a coefficient that is a universal amplitude \mathcal{A}_{χ_f} divided by the square of a nonuniversal velocity.

$$\chi_f = \frac{\mathcal{A}_{\chi_f}}{c^2} T. \quad (\text{C1})$$

We will set $c=1$ in the following. In general, we can think of the universal amplitude as a universal function $\mathcal{A}_{\chi_f} = \mathcal{A}_{\chi_f}(N_f, N_b)$ for arbitrary N_f, N_b . In the following, we will calculate this functional dependence at large N_f, N_b but for arbitrary values of the ratio N_b/N_f .

\mathcal{A}_{χ_f} at $N=\infty$. At $N=\infty$, we have a free theory of Dirac fermions and χ_f can be computed by simply evaluating the diagram in Fig. 8(a).

$$\begin{aligned} \chi_f &= -[\text{Tr}(T^a)^2] T \sum_{\omega_n} \int \frac{d^2 k}{4\pi^2} \text{Tr}(-i\omega_n + \vec{\sigma} \cdot \mathbf{k})^{-2} \\ &= 2[\text{Tr}(T^a)^2] \sum_{\omega_n} \int \frac{d^2 k}{4\pi^2} \frac{\omega_n^2 - k^2}{(k^2 + \omega_n^2)^2}. \quad (\text{C2}) \end{aligned}$$

We will evaluate the momentum integration first, using dimensional regularization, and then the frequency summation, using ζ -function regularization. It is easy to obtain the final answer by evaluating the frequency summation before the momentum integration, in which case no cutoff or regularization is needed. However, on including gauge fluctuations, it appears more convenient to perform the momentum inte-

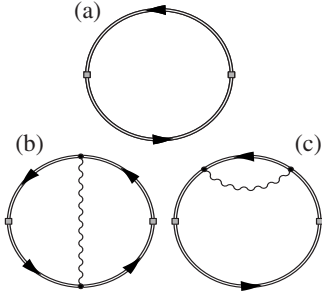


FIG. 8. Diagrammatic contributions to the susceptibility, χ_f , arising (a) at $N=\infty$ [(b) and (c)] at order $1/N$. All the diagrams give a linear- T dependence as expected for the susceptibility of a conserved charge for $z=1$ criticality in $d=2$ (Ref. 25).

gration first; this $N=\infty$ calculation then provides an opportunity to illustrate the method by which we regulate the frequency sums later on. Performing the momentum integration in d spatial dimensions, we obtain

$$\chi_f = [\text{Tr}(T^\alpha)^2] \frac{2(1-d)\Gamma(1-d/2)}{(4\pi)^{d/2}} T \sum_{\omega_n} |\omega|^{d-2}. \quad (\text{C3})$$

We evaluate the frequency summation using

$$g(s) = T \sum_{\omega_n} \frac{1}{|\omega_n|^s} = 2T^{1-s} \pi^{-s} (1-2^{-s}) \zeta(s). \quad (\text{C4})$$

From this, note that

$$T \sum_{\omega_n} 1 = g(0) = 0, \quad (\text{C5})$$

$$T \sum_{\omega_n} \ln |\omega_n| = - \left. \frac{dg}{ds} \right|_{s=0} = T \ln 2.$$

Using these results in Eq. (C3) in taking the limit $d \rightarrow 2$, we obtain

$$\chi_f = [\text{Tr}(T^\alpha)^2] \frac{T \ln 2}{\pi}. \quad (\text{C6})$$

\mathcal{A}_{χ_f} at next to leading order in $1/N$. We now turn to a

computation of the diagrams of Figs. 8(b) and 8(c); these are the only contributions to χ_f at next to leading order. As will be clear below, a full evaluation of these diagrams is not possible analytically. However, we will be able to achieve our main goal, which is to extract the numerical value of the $1/N$ corrections to the $N=\infty$ value of \mathcal{A}_{χ_f} computed above.

A direct evaluation of the two diagrams, Figs. 8(b) and 8(c) can be written in the form (including the $N=\infty$ result above)

$$\chi_f = [\text{Tr}(T^\alpha)^2] \left\{ D_1(0,0) + \frac{1}{N} T \sum_{\epsilon_n} \int \frac{d^2 k}{4\pi^2} \left[\frac{D_3(k, \epsilon_n)}{D_1(k, \epsilon_n)} - \frac{D_4(k, \epsilon_n)}{D_2(k, \epsilon_n) + (\epsilon_n^2/k^2)D_1(k, \epsilon_n)} \right] \right\},$$

$$D_3(\mathbf{k}, \epsilon_n) \equiv N_f T \sum_{\omega_n} \int \frac{d^2 q}{4\pi^2} \text{Tr} [2G_\Psi^3(\mathbf{q}, \omega_n) G_\Psi(\mathbf{q} + \mathbf{k}, \omega_n + \epsilon_n) + G_\Psi^2(\mathbf{q}, \omega_n) G_\Psi^2(\mathbf{q} + \mathbf{k}, \omega_n + \epsilon_n)],$$

$$D_4(\mathbf{k}, \epsilon_n) \equiv N_f T \sum_{\omega_n} \int \frac{d^2 q}{4\pi^2} \text{Tr} [2G_\Psi^3(\mathbf{q}, \omega_n) \sigma_i G_\Psi(\mathbf{q} + \mathbf{k}, \omega_n + \epsilon_n) \sigma_j + \epsilon_n \sigma_j + G_\Psi^2(\mathbf{q}, \omega_n) \sigma_i G_\Psi^2(\mathbf{q} + \mathbf{k}, \omega_n + \epsilon_n) \sigma_j] \times \left(\delta_{ij} - \frac{k_i k_j}{k^2} \right), \quad (\text{C7})$$

where the functions $D_{1,2}$ have been introduced (Sec. II B) and computed (Appendix A) before. Computations of $D_{3,4}$ are presented in Appendix D. We note here that the dependence of \mathcal{A}_{χ_f} on N_b enters through the N_b dependence of $D_{1,2}$. A full numerical evaluation of \mathcal{A}_{χ_f} was carried out and was found to reproduce the results of Sec. IV up to three significant digits.

APPENDIX D: EVALUATION OF D_3 and D_4

In this appendix, we summarize our strategy to evaluate the functions D_3 and D_4 defined in Eq. (C7). The techniques are similar to those used to evaluate $D_{1,2}$ and we will simply quote the final answers,

$$D_3(\mathbf{k}, \epsilon_n) = NT \sum_{\omega_n} \int \frac{d^2 q}{4\pi^2} \text{Tr} \{ 2(-i\omega_n + \vec{\sigma} \cdot \mathbf{q})^{-3} [-i(\omega_n + \epsilon_n) + \vec{\sigma} \cdot (\mathbf{q} + \mathbf{k})]^{-1} + (-i\omega_n + \vec{\sigma} \cdot \mathbf{q})^{-2} [-i(\omega_n + \epsilon_n) + \vec{\sigma} \cdot (\mathbf{q} + \mathbf{k})]^{-2} \}$$

$$= \frac{NT}{2\pi} \int_0^1 dx \sum_{\omega_n} \{ -2(x-1)\omega_n^4 - (x-1)(5x\epsilon_n + \epsilon_n)\omega_n^3 - (x-1)(2x^2k^2 - xk^2 - 2x^2\epsilon_n^2 + 7x\epsilon_n^2)\omega_n^2$$

$$- (x-1)(7k^2\epsilon_n x^3 - 3\epsilon_n^3 x^2 - 8k^2\epsilon_n x^2 + 3\epsilon_n^3 x + 3k^2\epsilon_n x)\omega_n - (x-1)[(x-1)x^2k^4 + 3x^3\epsilon_n^2 k^2 - 2x^2\epsilon_n^2 k^2 - x^2\epsilon_n^4] \}$$

$$\times \frac{(-1)}{[(1-x)\omega_n^2 + x(\omega_n + \epsilon_n)^2 + k^2 x(1-x)]^3}. \quad (\text{D1})$$

This last lengthy expression was generated in LATEX by MATHEMATICA, and also translated to FORTRAN by MATHEMATICA. The integral over x was evaluated numerically, and the frequency summation was performed using the following expansion at large ω_n :

$$-\frac{1}{\omega_n^2} - \frac{k^2 - \epsilon_n^2}{2\omega_n^4} + \frac{-k^4 + 7k^2\epsilon_n^2 - 2\epsilon_n^4}{6\omega_n^6}. \quad (\text{D2})$$

Similarly for D_4 , we have

$$\begin{aligned} D_4(\mathbf{k}, \epsilon_n) &= \left(\delta_{ij} - \frac{k_i k_j}{k^2} \right) NT \sum_{\omega_n} \int \frac{d^2 q}{4\pi^2} \text{Tr} \{ 2(-i\omega_n + \vec{\sigma} \cdot \mathbf{q})^{-3} \sigma_i [-i(\omega_n + \epsilon_n) + \vec{\sigma} \cdot (\mathbf{q} + \mathbf{k})]^{-1} \sigma_j \\ &\quad + (-i\omega_n + \vec{\sigma} \cdot \mathbf{q})^{-2} \sigma_i [-i(\omega_n + \epsilon_n) + \vec{\sigma} \cdot (\mathbf{q} + \mathbf{k})]^{-2} \sigma_j \} \\ &= \frac{NT}{2\pi} \int_0^1 dx \sum_{\omega_n} \{ -(1-3x)(x-1)\omega_n^4 - (x-1)(-10\epsilon_n x^2 + 3\epsilon_n x + \epsilon_n)\omega_n^3 \\ &\quad - (x-1)(-6k^2 x^3 - 8\epsilon_n^2 x^3 - k^2 x^2 - 7\epsilon_n^2 x^2 + 8k^2 x + 8\epsilon_n^2 x)\omega_n^2 \\ &\quad - (x-1)(-6k^2 \epsilon_n x^4 - 8\epsilon_n^3 x^3 + k^2 \epsilon_n x^3 + \epsilon_n^3 x^2 + 4k^2 \epsilon_n x^2 + 3\epsilon_n^3 x + 3k^2 \epsilon_n x)\omega_n \\ &\quad - (x-1)[x^2(x^3 - 4x^2 + 6x - 3)k^4 - 3x^4 \epsilon_n^2 k^2 + 6x^3 \epsilon_n^2 k^2 - 2x^2 \epsilon_n^2 k^2 - 2x^3 \epsilon_n^4 + x^2 \epsilon_n^4] \} \\ &\quad \times \frac{(-1)}{[(1-x)\omega_n^2 + x(\omega_n + \epsilon_n)^2 + k^2 x(1-x)]^3}. \end{aligned} \quad (\text{D3})$$

The frequency summand has the following expansion at large ω_n :

$$\frac{-2k^2 + \epsilon_n^2}{2\omega_n^4} + \frac{4k^4 - 17k^2 \epsilon_n^2 - \epsilon_n^4}{6\omega_n^6}. \quad (\text{D4})$$

-
- ¹G. R. Stewart, Rev. Mod. Phys. **56**, 755 (1984); **73**, 797 (2001).
²Y. Shimizu, K. Miyagawa, K. Kanoda, M. Maesato, and G. Saito, Phys. Rev. Lett. **91**, 107001 (2003).
³J. S. Helton, K. Matan, M. P. Shores, E. A. Nytko, B. M. Bartlett, Y. Yoshida, Y. Takano, A. Suslov, Y. Qiu, J.-H. Chung, D. G. Nocera, and Y. S. Lee, Phys. Rev. Lett. **98**, 107204 (2007).
⁴P. A. Lee, Rep. Prog. Phys. **71**, 012501 (2008).
⁵T. Senthil, A. Vishwanath, L. Balents, S. Sachdev, and M. P. A. Fisher, Science **303**, 1490 (2004); T. Senthil, L. Balents, S. Sachdev, A. Vishwanath, and M. P. A. Fisher, Phys. Rev. B **70**, 144407 (2004).
⁶Anders W. Sandvik, Phys. Rev. Lett. **98**, 227202 (2007).
⁷R. G. Melko and R. K. Kaul, Phys. Rev. Lett. **100**, 017203 (2008).
⁸F.-J. Jiang, M. Nyfeler, S. Chandrasekharan, and U.-J. Wiese, arXiv:0710.3926 (unpublished).
⁹N. Read and S. Sachdev, Phys. Rev. Lett. **62**, 1694 (1989); Phys. Rev. B **42**, 4568 (1990).
¹⁰M. Hermele, T. Senthil, M. P. A. Fisher, P. A. Lee, N. Nagaosa, and X.-G. Wen, Phys. Rev. B **70**, 214437 (2004); M. Hermele, T. Senthil, and M. P. A. Fisher, *ibid.* **72**, 104404 (2005).
¹¹R. K. Kaul, Y. B. Kim, S. Sachdev, and T. Senthil, Nat. Phys. **4**, 28 (2008).
¹²B. I. Halperin, T. C. Lubensky, and S.-k. Ma, Phys. Rev. Lett. **32**, 292 (1974).
¹³V. Yu. Irkhin, A. A. Katanin, and M. I. Katsnelson, Phys. Rev. B **54**, 11953 (1996).
¹⁴Flavio S. Nogueira and Hagen Kleinert, arXiv:cond-mat/0303485 (unpublished); F. S. Nogueira and H. Kleinert, in *Order, Disorder, and Criticality*, edited by Y. Holovatch (World Scientific, 2007).
¹⁵O. Vafek, Z. Tesanovic, and M. Franz, Phys. Rev. Lett. **89**, 157003 (2002).
¹⁶A. M. Polyakov, *Gauge Fields and Strings* (Harwood, Academic, Chur, Switzerland, 1987).
¹⁷Hagen Kleinert and Flavio S. Nogueira, Phys. Rev. B **66**, 012504 (2002).
¹⁸Olexei I. Motrunich and Ashvin Vishwanath, Phys. Rev. B **70**, 075104 (2004).
¹⁹Man-hot Lau and Chandan Dasgupta, Phys. Rev. B **39**, 7212 (1989).
²⁰Michael Kamal and Ganpathy Murthy, Phys. Rev. Lett. **71**, 1911 (1993).
²¹Shunsuke Takashima, Ikuro Ichinose, and Tetsuo Matsui, Phys. Rev. B **73**, 075119 (2006).
²²S. J. Hands, J. B. Kogut, L. Scorzato, and C. G. Strouthos, Phys. Rev. B **70**, 104501 (2004).
²³Shang-keng Ma, Phys. Rev. A **7**, 2172 (1973).
²⁴W. Rantner and X.-G. Wen, Phys. Rev. B **66**, 144501 (2002).
²⁵Andrey V. Chubukov, Subir Sachdev, and Jinwu Ye, Phys. Rev. B **49**, 11919 (1994).
²⁶S. Sachdev, Phys. Lett. B **309**, 285 (1993).
²⁷Oskar Vafek and Zlatko Tesanovic, Phys. Rev. Lett. **91**, 237001 (2003).
²⁸Patrick A. Lee, Naoto Nagaosa, and Xiao-Gang Wen, Rev. Mod. Phys. **78**, 17 (2006).
²⁹Ying Ran, Michael Hermele, Patrick A. Lee, and Xiao-Gang Wen, Phys. Rev. Lett. **98**, 117205 (2007).
³⁰Subir Sachdev, *Quantum Phase Transitions* (Cambridge University Press, Cambridge, 1999).